ELSEVIER

Physica B 323 (2002) 15–20

PHYSICA B

www.elsevier.com/locate/physb

Raman spectroscopy on one isolated carbon nanotube

M.S. Dresselhaus[a,b,*], A. Jorio[a,c], A.G. Souza Filho[a,d], G. Dresselhaus[e], R. Saito[f]

[a] *Department of Physics, MIT, Cambridge, MA 02139-4307, USA*
[b] *Department of Electrical Engineering and Computer Science, MIT, Cambridge, MA 02139-4307, USA*
[c] *Departamente de Fisica, Universidade Federal de Minas Gerais, Belo Horizonte, 30123-970 Brazil*
[d] *Departamente de Fisica, Universidade Federal de Ceará, Fortaleza, 60455-760 Brazil*
[e] *Francis Bitter Magnet Laboratory, MIT, Cambridge, MA 02139-4307, USA*
[f] *Department of Electronic Engineering, The University of Electro-Communications, Chofu, Tokyo, 182-8585, Japan*

Abstract

The use of Raman spectroscopy to elucidate the vibrational and electronic structure of single wall carbon nanotubes is reviewed. The special role played by single nanotube spectroscopy in the (n,m) structural characterization of individual nanotubes and in the elucidation of the spectra of nanotube bundles is emphasized.

PACS: 63.22.+m; 73.22.−f; 78.30.Na; 78.20.Bh

Keywords: Carbon nanotubes; Raman spectroscopy; D-band; Dispersive phonon mode

1. Introduction

Single wall carbon nanotubes are important nanostructures because of the new nanoscience concepts they have introduced. Some of these new concepts have been illuminated through Raman spectroscopy studies at the single nanotube level, and this is the focus of this review.

Raman spectroscopy provides an important characterization tool for carbon-based materials, showing different characteristic spectra for sp^3, sp^2 and sp carbons, as well as for disordered sp^2 carbons, fullerenes and carbon nanotubes. In particular, the Raman spectra for single wall carbon nanotubes (SWNTs) are unique, distinctive and different from the spectra for other carbons, because of the strong enhancement of the Raman effect when the laser excitation energy is in resonance with interband transitions between sharp singularities in the 1D electronic density of states in the valence and conduction bands of the nanotubes [1]. Raman spectroscopy thus provides unique information about both the vibrational and electronic properties of SWNTs.

Each SWNT is characterized by two integers (n,m), which specify the number of unit vectors $\vec{a}_1$ and $\vec{a}_2$ in the graphene honeycomb structure [2]. These (n,m) indices also constitute the chiral vector (or roll-up vector) $\vec{C}_h = n\vec{a}_1 + m\vec{a}_2$ corresponding to the nanotube circumference, and these two indices determine the nanotube diameter and chirality, or the orientation of the carbon

*Corresponding author. Department of Electrical Engineering and Computer Science, Massachusetts Institute of Technology, 77 Massachusetts Avenue, Room 13-3005, 02139-4307 Cambridge, MA, USA. Tel.: +1-617-253-6864; fax: +1-617-253-6827.

E-mail address: millie@mgm.mit.edu (M.S. Dresselhaus).

0921-4526/02/$ - see front matter
PII: S0921-4526(02)00873-6

hexagons with respect to the nanotube axis. The electronic properties of SWNTs are remarkable insofar as they can be either metallic (when $m - n = 3q$, where q is an integer) or semiconducting (when $n - m = 3q \pm 1$), depending simply on the nanotube geometry [3].

In this paper we review how the Raman effect provides unique information about the vibrational and electronic properties of SWNT bundles and how the observation of individual nanotubes, not only provides unique and important information about the vibrational and electronic properties, but also determines the structural (n,m) properties of individual nanotubes [4]. This information is further used to determine, to high resolution, the profile of the density of states near a singularity in the electronic joint density of states [5]. Because of the high sensitivity of the electronic, transport, vibrational and other nanotube properties to the structural (n,m) indices, this non-destructive, readily available characterization technique is expected to have a significant impact on current basic research on carbon nanotubes. In this paper we also discuss the relation between the spectra of SWNT bundles and the spectra for single isolated SWNTs.

2. Raman spectra from SWNT bundles

Raman spectroscopy in SWNTs exhibits a new physical phenomenon, called diameter-selective resonance Raman scattering, whereby only those (n,m) nanotubes, that have interband transitions that are within the resonant window of the excitation laser E_{laser}, exhibit Raman spectra that are intense enough to be observable. Of particular significance is the radial breathing mode (RBM) as in Fig. 1, which is a feature unique to carbon nanotubes relative to other sp^2 carbons, where all the atoms in the nanotube are vibrating in phase in the radial direction. Since the RBM frequency ω_{RBM} is proportional to the inverse nanotube diameter $(1/d_t)$, Raman spectroscopy has become a characterization tool for the determination of the SWNT diameter for the small subset of SWNTs that are in resonance with E_{laser} [1]. By measurement of ω_{RBM} for many laser energies E_{laser}, the diameter distribution of the nanotubes in a particular SWNT bundle can be found, and in this way Raman spectroscopy has become a dominant characterization method for the nanotube diameter distribution. Raman spectroscopy can also be used to distinguish between metallic

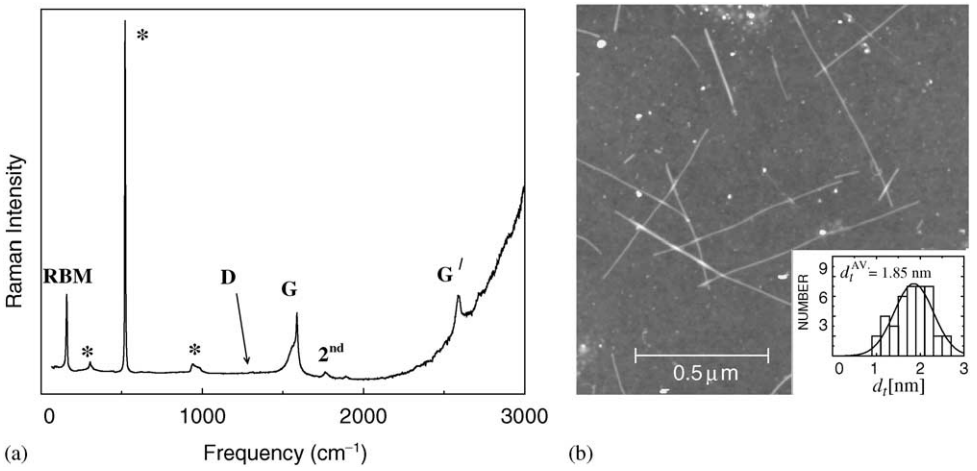

Fig. 1. (a) Raman spectrum from one nanotube taken over a broad frequency range using $E_{\text{laser}} = 785$ nm $= 1.58$ eV excitation, and showing the RBM, the D-band, the G-band, second-order features and the G′-band. The features marked with '$*$' at 303, 521 and 963 cm^{-1} [6] are from the Si/SiO_2 substrate and are used for calibration of the nanotube Raman spectrum. (b) AFM image of the sample showing isolated SWNTs grown from the vapor phase [7]. The small particles are iron catalyst particles. The inset shows the diameter distribution of this sample based on the AFM observations of 40 SWNTs [4].

and semiconducting nanotubes because of their different G-band lineshapes [1].

The highly dispersive D-band and its second harmonic G′-band, which are commonly seen in sp^2 carbons, are also observed in SWNT bundles, except that superimposed on the linear dependence of ω_D and $\omega_{G'}$ on E_{laser}, which is characteristic of sp^2 carbons, is an oscillatory feature in SWNT bundles [8]. This behavior can be explained from studies at the single nanotube level [9].

3. Single nanotube spectroscopy

The very large density of electronic states for 1D systems at their van Hove singularities and the strong electron–phonon coupling under resonance conditions allows observation of the Raman spectra from one individual SWNT when the incident or scattered photon is in resonance with a valence to conduction band interband transition E_{ii} between van Hove singularities. As shown in Fig. 1, these isolated nanotube spectra exhibit all the Raman features normally observed in SWNT bundles. The presence of Raman lines from the substrate allows a calibration to be made of the Raman intensities of each feature in the single nanotube spectrum (see Fig. 1). Near resonance, the intensity of the features from an isolated nanotube can be as large as the features from the Si substrate.

The analysis of all resonance Raman effects has been greatly aided by the introduction by Kataura et al. of a plot [see Fig. 2(a)] of the interband transitions E_{ii} as a function of d_t for all values of (n,m) [10], showing that each (n,m) nanotube has a unique set of E_{ii} transition energies, which is physically due to the trigonal warping effect of the constant energy contours for a graphite sheet [11,13]. The resonance Raman effect using one laser line allows determination of an E_{ii} value to about 10 meV accuracy from measurement of the relative intensities of the RBM Stokes and anti-Stokes components [14], while the nanotube diameter is found from the RBM frequency, as mentioned above. Thus using the Kataura plot relating each (n,m) nanotube to its E_{ii} value, we can determine the (n,m) values of individual nanotubes from their E_{ii} values [4].

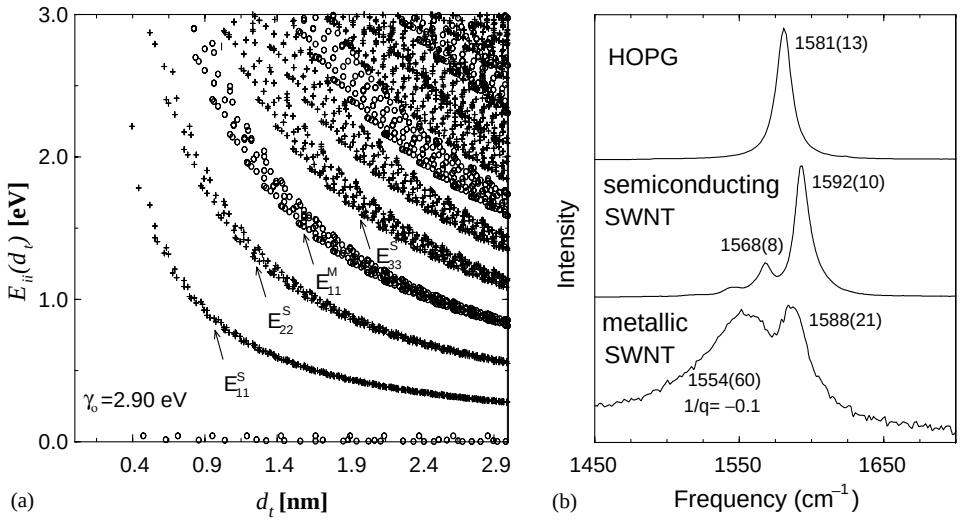

Fig. 2. (a) Calculated [10] energy separations $E_{ii}(d_t)$ between van Hove singularities i in the 1D electronic density of states of the conduction and valence bands for all (n,m) values vs nanotube diameter $0.4 < d_t < 3.0$ nm, using a value for the carbon–carbon energy overlap integral of $\gamma_0 = 2.9$ eV and a nearest neighbor carbon–carbon distance $a_{C-C} = 1.42$ Å [11,12]. Semiconducting (S) and metallic (M) nanotubes are indicated by crosses and open circles, respectively. The index i in the interband transitions E_{ii} denotes the transition between the van Hove singularities, with $i = 1$ being closest to the Fermi level. (b) G-band spectra for highly oriented pyrolytic graphite (HOPG), an isolated semiconducting nanotube and an isolated metallic nanotube. The frequencies (linewidths) for each of the characteristic features are given, including the asymmetry parameter $1/q$ for the Breit–Wigner–Fano line at 1554 cm^{-1}.

The self-consistent identification of (n,m) for a large number of nanotubes, based on the relative intensities of the radial breathing mode for SWNTs lying within the resonant window of $E_{\text{laser}} \pm 0.1$ eV, yields the proportionality factor $\alpha = 248\ \text{cm}^{-1}\ \text{nm}$ in the relation $\omega_{\text{RBM}} = \alpha/d_t$. This value of α then forms the basis for subsequent (n,m) identification of isolated SWNTs on Si/SiO_2 substrates [4]. The actual width of the van Hove singularities in the electronic density of states was determined from measurement of the dependence on the Stokes and anti-Stokes intensities on E_{laser} over the resonant window of an individual SWNT [5].

We have used the (n,m) indices of an isolated SWNT, thus determined, to study the dependence of each of the features [see Fig. 1(a)] of the single nanotube spectra (including their frequencies, linewidths and intensities) on nanotube diameter d_t, chiral angle θ, and laser excitation energy E_{laser} and intensity. Some of the features, such as the dependence of ω_{G} on d_t [15] and the appearance of a double peak structure in the G′-band [16], provide an internal check on the (n,m) assignment, that was made by the analysis of the RBM [4], as discussed above. These two phenomena are, however, interesting in their own right. For example, the G-band in isolated nanotubes shows two strong features [see Fig. 2(b)], with the higher frequency component ω_{G}^{+} being essentially independent of d_t and the lower frequency component ω_{G}^{-} decreasing in frequency, in accordance with $\omega_{\text{G}}^{-} = \omega_{\text{G}}^{+} - \mathscr{C}/d_t^2$ where $\mathscr{C} = 47.7\ \text{cm}^{-1}\ \text{nm}^2$ for semiconducting nanotubes and $\mathscr{C} = 79.5\ \text{cm}^{-1}\ \text{nm}^2$ for metallic nanotubes [15].

By carrying out measurements at the single nanotube level the $\omega_{\text{G}}(d_t)$ dependence is clearly revealed and helps to understand the G-band lineshape of SWNT bundles, which have a distribution of nanotube diameters, but do show two dominant features whose spacing depends on the mean diameter of the SWNT bundle [1]. The insensitivity of ω_{G}^{+} to d_t could be understood in terms of vibrations along the nanotube axes where the bond lengths are not dependent on nanotube curvature and hence not on d_t. In contrast, vibrations associated with ω_{G}^{-} are with bonds in the circumferential direction, and these are expected to show mode-softening effects due to the admixture of out-of-plane graphite modes arising from nanotube curvature, which increase as d_t decreases according to an inverse d_t^2 dependence. Likewise, the complex structure of the RBM band for an SWNT bundle can be understood in terms of a superposition of simple Lorentzian contributions at the single nanotube level, but weighted appropriately by the number of each (n,m) nanotube in resonance with E_{laser}, by each tube length in the light spot, and by a resonance profile factor that depends on the energy separation $E_{\text{laser}} - E_{ii}$.

Moreover, observations at the single nanotube level also allow new physics to be investigated, such as can be observed through the large dispersion of the G′-band with E_{laser}, permitting the observation of resonance of the incident photon E_{laser} with one van Hove singularity (e.g., E_{44}^{S}) and the scattered photon $E_{\text{laser}} - \hbar\omega_{\text{G}'}$ with another van Hove singularity (e.g., E_{33}^{S}). For nanotube bundles, it is often difficult to separate contributions from resonances with the incident and scattered photons, but these distinctions can much more easily be observed at the single nanotube level.

Observations for SWNT bundles are also valuable because they allow study of the dispersive D-band and G′-band effects in SWNT bundles, which show superposition of an oscillatory component due to resonance of E_{laser} with specific van Hove singularities on top of the linear ω_{D} and $\omega_{\text{G}'}$ dependence on E_{laser} associated with sp^2 carbons [see Fig. 3(a)]. On the other hand, the detailed explanation of the oscillatory components associated with the SWNT van Hove singularities [Fig. 3(b)] requires an understanding of the specific phonon q-vector which are in resonance with the electron wave vectors k_{ii} at the van Hove singularities for nanotubes in a given electronic transition E_{ii} [see Fig. 3(c)]. Each nanotube with an E_{ii} within the resonant window of a particular E_{laser} excitation energy corresponds to specific phonon q-vectors and their corresponding frequencies $\omega_{\text{D}}(d_t)$ and $\omega_{\text{G}'}(d_t)$ which depend on the nanotube diameter. Resonance Raman spectroscopy at the single nanotube level has thus worked hand in hand with the spectroscopy of SWNT

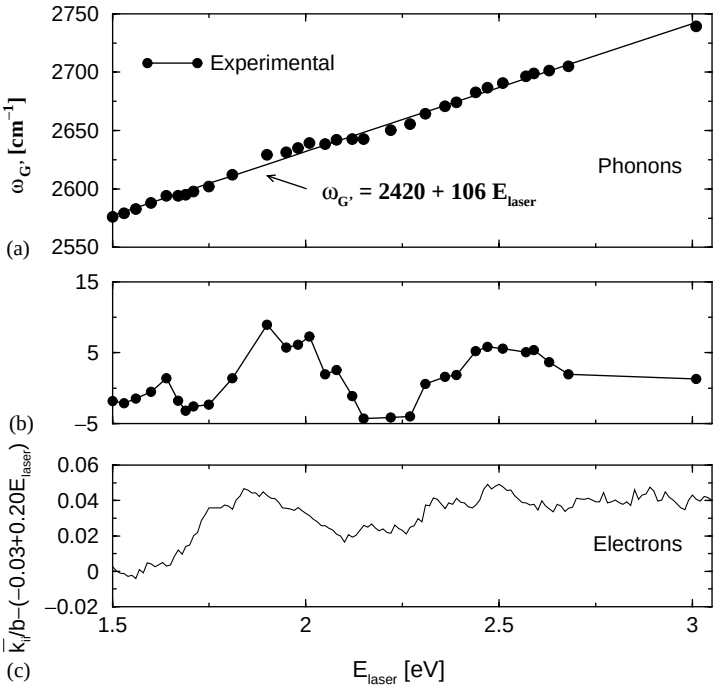

Fig. 3. (a) Dependence on the laser excitation energy of $\omega_{G'}$ for the dominant second-order Raman feature for SWNT bundles. In contrast to most sp^2 carbons where $\omega_{G'}$ depends linearly on E_{laser}, the corresponding plot for SWNT bundles shows a superimposed step-like or oscillatory behavior near 2.0 and 2.5 eV for SWNT bundles. (b) The oscillatory component of (a) obtained after subtracting the linear background given by $\omega_{G'} = 2420 + 106E_{laser}$ in (a). (c) Plot of the E_{laser} dependence of the oscillations in the resonant electron wave vector k_{ii} after normalization to the length of the basis vector b of the reciprocal lattice of 2D graphite and after subtracting the linear background. The strong correspondence between the E_{laser} dependence of $\omega_{G'}$ for phonons and $\bar{k}_{ii}$ for electrons provides support at the single nanotube level for the identification of each oscillation with a particular interband transition between van Hove singularities, as is observed for nanotube bundles [17].

bundles, revealing the underlying physics responsible for various features in the Raman spectra, as well as providing detailed information about many aspects of the vibrational and electronic properties of carbon nanotubes. The use of Raman spectroscopy as a characterization tool for individual nanotubes is expected to open up many new opportunities for the exploration of the dependence of the remarkable physical properties of carbon nanotubes on their diameter and chirality.

Acknowledgements

R.S. acknowledges a Grant-in-Aid (No. 13440091) from the Ministry of Education, Japan. A.J./A.G.S.F. acknowledge support from the Brazilian agencies CNPq/CAPES. The MIT authors acknowledge support under NSF Grants DMR 01-16042, INT 98-15744, and INT 00-00408.

References

[1] M.S. Dresselhaus, P.C. Eklund, Adv. Phys. 49 (2000) 705.
[2] R. Saito, G. Dresselhaus, M.S. Dresselhaus, Physical Properties of Carbon Nanotubes, Imperial College Press, London, 1998.
[3] R. Saito, M. Fujita, G. Dresselhaus, M.S. Dresselhaus, Appl. Phys. Lett. 60 (1992) 2204.
[4] A. Jorio, R. Saito, J.H. Hafner, C.M. Lieber, M. Hunter, T. McClure, G. Dresselhaus, M.S. Dresselhaus, Phys. Rev. Lett. 86 (2001) 1118.

[5] A. Jorio, A.G. Souza Filho, G. Dresselhaus, M.S. Dresselhaus, R. Saito, J.H. Hafner, C.M. Lieber, F.M. Matinaga, M.S.S. Dantas, M.A. Pimenta, Phys. Rev. B 63 (2001) 245.
[6] P.A. Temple, C.E. Hathaway, Phys. Rev. B 7 (1973) 3685.
[7] J.H. Hafner, C.L. Cheung, T.H. Oosterkamp, C.M. Lieber, J. Phys. Chem. B 105 (2001) 743.
[8] M.A. Pimenta, E.B. Hanlon, A. Marucci, P. Corio, S.D.M. Brown, S.A. Empedocles, M.G. Bawendi, G. Dresselhaus, M.S. Dresselhaus, Brazilian J. Phys. 30 (2000) 423.
[9] M.S. Dresselhaus, G. Dresselhaus, A. Jorio, A.G. Souza Filho, R. Saito, unpublished.
[10] H. Kataura, Y. Kumazawa, Y. Maniwa, I. Umezu, S. Suzuki, Y. Ohtsuka, Y. Achiba, Synth. Met. 103 (1999) 2555.
[11] R. Saito, G. Dresselhaus, M.S. Dresselhaus, Phys. Rev. B 61 (2000) 2981.
[12] G. Dresselhaus, M.A. Pimenta, R. Saito, J.-C. Charlier, S.D.M. Brown, P. Corio, A. Marucci, M.S. Dresselhaus, in: D. Tománek, R.J. Enbody (Eds.), Science and Applications of Nanotubes, 2000, Proceedings of the International Workshop on the Science and Applications of Nanotubes, Michigan State University, East Lansing, MI, USA, Kluwer Academic, New York, July 24–27, 1999, pp. 275–295.
[13] T.W. Odom, J.L. Huang, P. Kim, C.M. Lieber, Nature (London) 391 (1998) 62.
[14] A.G. Souza Filho, A. Jorio, J.H. Hafner, C.M. Lieber, R. Saito, M.A. Pimenta, G. Dresselhaus, M.S. Dresselhaus, Phys. Rev. B 63 (2001) 241404R.
[15] A. Jorio, A.G. Souza Filho, G. Dresselhaus, M.S. Dresselhaus, A.K. Swan, B.B. Goldberg, M.S. Ünlü, M.A. Pimenta, J.H. Hafner, C.M. Lieber, R. Saito, Phys. Rev. B 65 (2002) 155412.
[16] A.G. Souza Filho, A. Jorio, G. Dresselhaus, M.S. Dresselhaus, A.K. Swan, M.S. Ünlü, B.B. Goldberg, R. Saito, J.H. Hafner, C.M. Lieber, M.A. Pimenta, MRS Symposium Proceedings, vol. 706, Z6.17 (2001).
[17] A.G. Souza Filho, A. Jorio, G. Dresselhaus, M.S. Dresselhaus, R. Saito, A.K. Swan, M.S. Ünlü, B.B. Goldberg, J.H. Hafner, C.M. Lieber, M.A. Pimenta, Phys. Rev. B 65 (2002) 03544.